ab-initio study on Schottky-barrier modulation in $NiSi_2$/Si interface

Jiseok Kim*, Byounghak Lee†, Yumi Park†, Kota V R M Murali†, Francis Benistant‡,
*GLOBALFOUNDRIES, Albany, NY 12203, USA, jiseok.kim@globalfoundries.com
†GLOBALFOUNDRIES, Malta, NY 12020, USA
‡GLOBALFOUNDRIES, Singapore 528830, Singapore

***Abstract*—Interface morphology dependent Schottky Barrier Height (SBH) and its modulation by substitutional dopants in $NiSi_2$/Si interface have been investigated using density functional theory. An accurate band gap of Si was estimated by employing meta-GGA exchange correlation functional. We show that the SBH for electrons (in n-type semiconductor) is significantly lower for (001) than (111) orientation of Si. These results are in qualitative agreement with experimental results on interface morphology dependent SBH. Also, we show that the SBH can be significantly reduced by substitutional dopants near the $NiSi_2$/Si interfaces. An optimization of the SBH through dopant location, dopant type and orientation of Si is discussed.**

I. Introduction

A reduction of the Schottky Barrier Height (SBH) (or equivalently the reduction of contact resistivity) at the metal-semiconductor (M-S) interfaces has become a key issue for the next generation semiconductor technology development. The source or drain contact resistance has become a dominant component of parasitic resistance of MOSFET devices to maintain high drive current [1]. It is known that the SBH is determined by the metal Fermi-level (FL) pinning to the charge neutrality level (CNL) of the interface states due to metal-induced gap states (MIGS). These are a continuum of energy states around FL that arise due to exponential decay of metal wavefunction into the semiconductor [2], [3]. This simple model of SBH, within the framework of CNL, has been widely used due to its simplicity while leaving out specific details of chemical bonding at the interface [3], [4]. However, in contrast to this existing view, Tung *et. al.*, suggested an intrinsic SB formation mechanism based on the local interface-related electronic structure and the interface morphology dependent SBH at the M-S interfaces. This mechanism has been corroborated through various experimental studies [5]–[8]. Since then, a variety of studies have been carried out to understand specific details of atomistic structure of a M-S interfaces in order to find a favorable interface morphology and composition to lower the SBH. In addition to the interface morphology engineering, dopant segregation or shallow implant technique at the M-S interfaces has been proposed to reduce the SBH. These techniques have shown improved electrical performances in MOSFET devices [9]–[11]. While the SBH reduction effect by dopant segregation and shallow implant techniques have been phenomenological explained in many experimental studies, the physical mechanisms responsible for the barrier height modulation are yet to be clearly understood.
Density functional theory (DFT) is a powerful technique to understand SB formation and the modulation of the SBH through interface, composition, or doping engineering at the M-S interfaces [8], [12]–[14]. The SBH for $NiSi_2$/Si has has drawn particular interest because of its extensive use in M-S contacts and also due to its well defined interface structure [7], [12]–[14]. However, many of the previous DFT studies on $NiSi_2$/Si interfaces had a drawback of band gap underestimation, with local density approximation (LDA) or generalized gradient approximation (GGA) or limited to the supercell slab model, with slab thicknesses smaller than the depletion width and with moderate doping density.
In this paper, we have theoretically investigated the interface orientation dependent SBH and its modulation at $NiSi_2$/Si(001) and $NiSi_2$/Si(111) interfaces by substitutional dopants using DFT with semi-infinite electrodes by applying open boundary conditions as implemented in the Atomistix Toolkit (ATK) [15], [16].

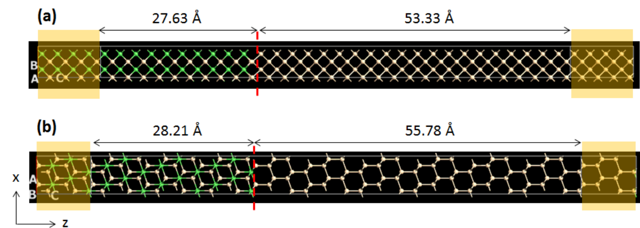

Fig. 1. Relaxed atomistic configurations of (a) $NiSi_2$/Si(001) and (b) $NiSi_2$/Si(111) interfaces which are periodic along x-y plane and semi-infinite along the z-direction with left and right electrodes represented by shaded rectangular boxes. The vertical dotted lines indicate the interfaces.

II. Methodology

The DFT calculations, in this paper, have been performed using the Atomistix Toolkit(ATK) code with localized (numeric atom centered) basis sets and norm conserving pseudopotentials. We have used meta-GGA (MGGA) [17] for the exchange correlation functional with calibrated $c = 1.0815$ parameter to obtain an accurate band gap of silicon (Si) (E_g=1.12 eV). In order to get converged results, a cutoff energy of 75 Hartree and Monkhorst-Pack k-point sampling of $11\times11\times100$ were used.
Figure 1 shows the simulated atomistic configurations of intrinsic $NiSi_2$/(001)Si and $NiSi_2$/(111)Si interfaces with semi-infinite left and right electrodes with Neumann boundary conditions. A atomic geometry optimization has been performed using GGA for a computational efficiency and the Limited-memory Broyden-Fletcher-Goldfarb-Shanno (L-BFGS) as im-

978-1-4673-7860-4/15/$31.00 ©2015 IEEE

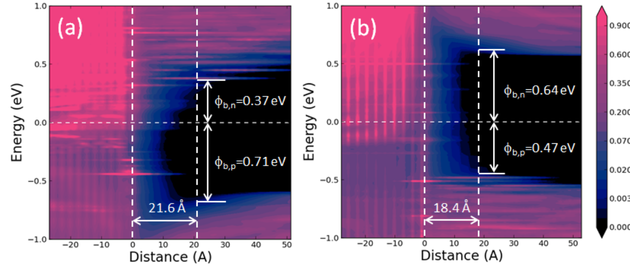

Fig. 2. Contour plots of LDOS of intrinsic (a) $NiSi_2$/(001)Si and (b) $NiSi_2$/(111)Si where the interface between the $NiSi_2$ and Si is located at z=0. SBH is extracted at z=21.6 $\AA$ and z=18.4 $\AA$ away from the interface for (a) and (b), respectively, where the LDOS at the Fermi level becomes small enough. Extracted SBHs for electrons and holes are denoted as $\phi_{b,n}$ and $\phi_{b,p}$, respectively.

plemented in ATK with the maximum force tolerance of 0.02 eV/$\AA$. The interlayer distance between $NiSi_2$ and Si layers was also optimized to minimize total energy. Note that the length of the Si region is larger than the depletion width (~40$\AA$) in the case of highly doped Si (>5×10^{19}cm^{-3}).

Once we have obtained the fully optimized geometry, we calculate the local density of states (LDOS) to extract the SBH at the interface. However, we would like to point out that the SBH extraction from the LDOS may not be very accurate because the barrier height is determined by arbitrary criteria when reading the LDOS which would be discussed in more details in the following section.

III. Results and Discussions

Figure 2 shows the contour plots of LDOS for intrinsic configurations as shown in Fig. 1 under zero bias condition. We have determined the SBH for electrons ($\phi_{b,n}$) and holes ($\phi_{b,p}$) at $\sim$ 20 $\AA$ away from the interface for both configurations where the LDOS (or metal-induced-gap-states (MIGS) density) at the FL (referenced to zero energy) becomes negligibly small (*i.e.* LDOS(E=E_F) $<10^{-4}$ in arbitrary unit). The MIGS density can be seen more clearly in Fig. 3 (a) where the LDOS is plotted as a function of energy at the interface z=0. This MIGS density near the interface is attributed to the valence electrons in d-orbital of Ni atom rather than Si as shown in Fig. 3 (b) where the atom projected DOS (PDOS) is plotted for Ni and Si atoms near the interface. However, as mentioned above, the criteria (LDOS(E=E_F) $<10^{-4}$) for the MIGS density is purely arbitrary because there is no certain criteria or consensus on how much of the LDOS at FL would be small 'enough' at which the SBH is extracted. Thus, we have used the criteria 10^{-4} so that the sum of the $\phi_{b,n}$ and $\phi_{b,p}$ becomes close to the bulk band gap of Si near the interface. This is why we have extracted SBH at different z-coordinates from the the interface between the 'relaxed' and 'unrelaxed' cases as shown in Fig. 3 (c) in which we have found that the SBH is slightly modified after the geometry relaxation.

Even though there exists an inevitable ambiguity in the SBH extraction using the LDOS, the extracted SBHs $\phi_{b,n}$=0.37 eV ($\phi_{b,p}$=0.71 eV) and $\phi_{b,n}$=0.64 eV ($\phi_{b,p}$=0.47 eV) for $NiSi_2$/Si(001) and $NiSi_2$/Si(111) interfaces respectively, agrees surprisingly well with experiments by Tung *et. al.* as shown in Refs [5], [6] in which they reported $\phi_{b,n}$=0.38~0.4 eV

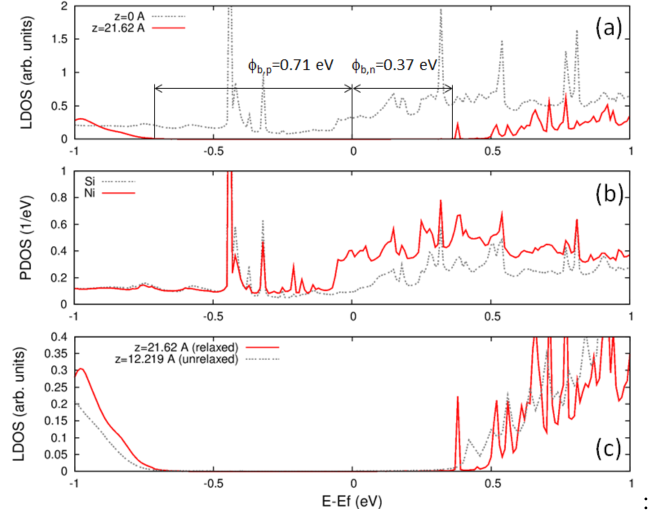

Fig. 3. LDOS and PDOS for intrinsic $NiSi_2$/(001)Si. (a) LDOS at the interface (dotted line) and z=21.62$\AA$ away from the interface (solid line). (b) Atom projected DOS for Si (dotted line) and Ni (solid line) atoms near the interface. (c) LDOS at z=21.62$\AA$ and z=12.22$\AA$ away from the interface with (solid line) and without (dotted line) geometry relaxation, respectively.

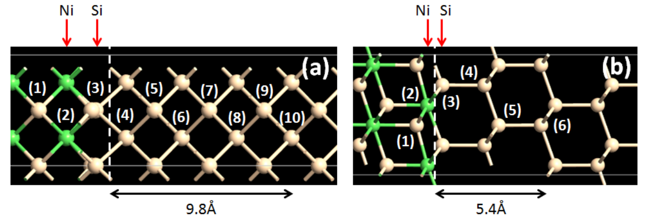

Fig. 4. Various substitutional dopant sites as numbers near (a) $NiSi_2$/(001)Si and (b) $NiSi_2$/(111)Si interfaces. The interface location is indicated by vertical dashed line.

(±0.02 eV) and $\phi_{b,p}$=0.68~0.73 eV (±0.02 eV) for uniform $NiSi_2$/(001)Si and $\phi_{b,n}$=0.65 eV (±0.01 eV) for type-A $NiSi_2$/Si(111). This remarkably good agreement for both n-type and p-type barrier heights with experiments can be attributed to the MGGA exchange correlation functional with well calibrated c-parameter to the bulk band gap of Si. Gao *et. al.* also employed Heyd-Scuseria-Ernzerhof (HSE) screened exchange hybrid functionals to overcome the band gap underestimation problem of LDA or GGA [14]. They demonstrated the morphology and metallic property dependent SBH but the reported SBH is $\phi_{b,n}$=0.52 eV for $NiSi_2$/(001)Si, which is slightly larger than one from Tung's experiment.

It should be noted that our calculated results strongly support the interface morphology dependent SBH from experiments which cannot be explained by CNL model as a bulk property of semiconductors. Also note the SBH from an ideal Mott-Schottky theorem ($\phi_{b,n} = \Phi_M - \chi_x = 5.03\ eV - 4.05\ eV = 0.98\ eV$) is not valid and the significant deviation from the ideal SBH to our results can be qualitativley explained by the interface dipole moments. The formation of the interface dipole can be seen in Fig. 5 (c) and (d) in which we show the macroscopic average of the electron difference density, $n(z) = n_{\text{SCF}}(z) - n_{\text{atom}}(z)$, where $n_{\text{SCF}}(z)$ is the total electron density from our DFT calculations and $n_{\text{atom}}(z)$ is the sum

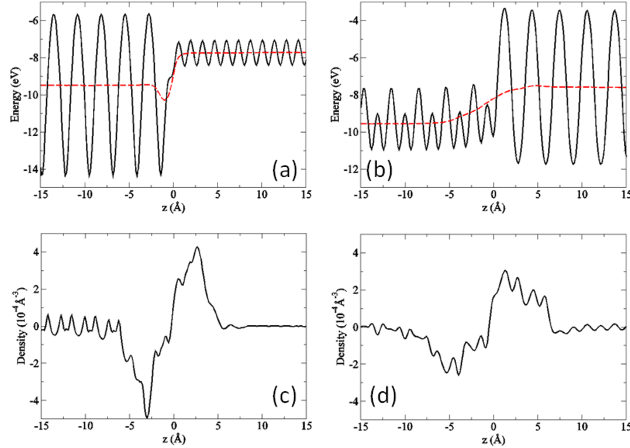

Fig. 5. The effective local electrostatic potentials $V(z)$ in (a) and (b), and the average electron difference density in (c) and (d), for $NiSi_2$/(001)Si and $NiSi_2$/(111)Si, respectively. In (a) and (b), the dashed line is the macroscopic average of $V(z)$.

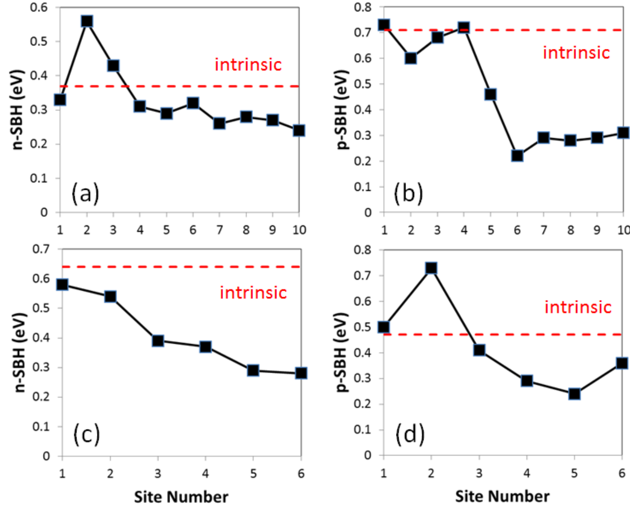

Fig. 6. $\phi_{b,n}$ and $\phi_{b,p}$ modulation in (a) and (b) for $NiSi_2$/(001)Si, and in (c) and (d) for $NiSi_2$/(111)Si, respectively, by substitutional As and B at site numbers indicated in Fig. fig4 where the intrinsic $\phi_{b,n}$ and $\phi_{b,p}$ from Fig. 2 is referenced as dashed horizontal line.

of the atomic electron density. The macroscopic avarage of $n(z)$ is zero in the electrically unpolarized region while it is non-zero when the electric dipole moment is present. It clearly shows that the larger shift of the electrostatic potential and consequently the larger modification of the SBH in the $NiSi_2$/(001)Si interface is due to the larger interface dipole moment. As a results of the larger interface dipole in Fig. 5 (c) for $NiSi_2$/(001)Si, the Fig. 5 (a) shows a steeper change in the electrostatic ponteital, *i.e.* a stronger electric field when compared to the $NiSi_2$/(111)Si as shown in 5 (b).

Having discussed the interface morphology dependent SBH, we study the SBH modulation by substitutional dopant segregation. Figure 4 shows the substitutional dopant sites labeled by numbers for (a) $NiSi_2$/(001)Si and (b) $NiSi_2$/(111)Si. We have replaced either Ni (at site (2)) or Si (at the rest of the sites

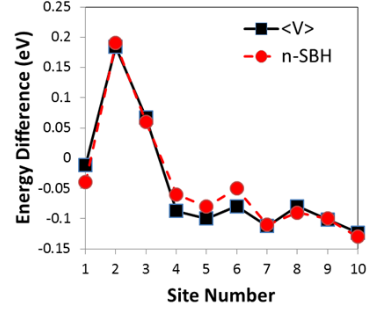

Fig. 7. Relative shifts of electrostatic difference potential (square with solid line) and $\phi_{b,n}$ (circle with dashed line) from the intrinsic case for the $NiSi_2$/(001)Si by the substitutional As at sites number (1)∼(10).

(1, 3-10)) by n-type (Arsenic) and p-type (Boron) dopants near the $NiSi_2$ and Si interfaces which correspond to the doping density of 5.95×10^{20} cm^{-3} for (001)Si and 7.14×10^{20} cm^{-3} for (111)Si. LDOS calculation for SBH extraction as well as the interface geometry relaxation have been performed in a same way as described above. Figure 6 show the n-type and p-type SBH modulation by the substitutional As and B atoms at the sites indicated in Fig. 4 for $NiSi_2$/Si(001) and $NiSi_2$/Si(111), respectively. Note that the subsitutional sites are extended up to 9.8$\AA$ and 5.4$\AA$ away from the interface of $NiSi_2$/Si(001) and $NiSi_2$/Si(111), respectively, which are far enough distances compared to the depletion width of 1.37 nm and 1.27 nm for the corresponding doping concentrations. As clearly seen in Fig 6 (a) and (b) for $NiSi_2$/(001)Si, the $\phi_{b,n}$ by As substitution (or segregation) is reduced by ∼35% at site number 10 (9.8$\AA$ away from the interface) and the $\phi_{b,p}$ by B substitution is reduced by ∼69% at site number 6 (2.7$\AA$ away from the interface). Interestingly, the $\phi_{b,n}$ is increased when the As dopant substitutes the Ni atom at site number 2 but the reduced $\phi_{b,p}$ is seen when the Ni is replaced by the B dopant. A similar trend is also observed for $NiSi_2$/(111)Si as shown in Fig. 6 (c) and (d) in which we show ∼56% and ∼49% reduction in $\phi_{b,n}$ and $\phi_{b,p}$, respectively, from the intrinsic case. Note that the n-type SBH reduction by As substitution is more significant with (111) Si while the p-type SBH reduction by B substitution is more significant with (001) Si. In other words, the SBH modulation by the substitutaional dopants also depends on the interface orientation or morphology.

The reduction (or change) of the SBH by the dopant substitution can be attributed to the modification of the electrostatic potentials. We have compared the relative shifts of the SBH to the shifts of the electrostatic potential from the intrinsic case as shown in Fig. 7. We have calculated the plane averaged electrostatic difference potential for the comparison which is a solution of the Poisson's equation for the electron difference density $n(z)$. As seen in Fig. 7, the shifts of the SBH matches to the shifts of the electrostatic potentials which is due to compensated intrinsic interface dipole moments by the As-induced dipole as discussed in Ref. [13].

Also the induced image charge on the $NiSi_2$ side due to the excess valence electron by As substitution in Si side is partially responsible to a reduction of $\phi_{b,n}$ [18]. The image force barrier lowering for the n-type SBH from the semi-classical

electrostatics without atomistic details is given as [20],

$$\Delta\phi_{b,n} = q\left[\frac{q^3 N_D(V_{bi} - V)}{8\pi^2\epsilon_s^3}\right]^{1/4}, \quad (1)$$

where the N_D is the donor doping density in the semiconductor, ϵ_s=11.7ϵ_0 is the dielectric constant of the Si, V is the applied voltage to the contact which is assumed to be very small ($< 10^{-5}$), and $qV_{bi} = \phi_n - (E_c - E_{FS})$ is the surface potential where the position of the conduction band E_c relative to the Fermi-level E_{FS} is approximated as shown in Ref. [19]. We have estimated the $\Delta\phi_{b,n} = 0.36\ eV$ and $0.42\ eV$ for (001)Si and (111)Si, respecitvely, corresponding to the doping densities above mentioned. Thus, the SBH with the image force barrier lowering effect becomes $\phi_{b,n}(= \phi_{b,n0} - \Delta\phi_{b,n} = 0.37 - 0.36) = 0.01\ eV$ and $\phi_{b,n} = 0.22\ eV$ for (001) Si and (111) Si, respecitvely, where the $\phi_{b,n0}$ is the SBH from the intrinsic $NiSi_2$/Si interfaces in Fig 2. It is clear that the SBHs from the convetional image force barrier lowering model deviate significantly (especially for the (001) Si) from the dopant site dependent SBH as shown in Fig. 6. Because it lacks the atomistic configuration details and associated electronic structure near the interface as well as the information on the dopant positions. So, our results on the SBH reduction by substitutional dopants cannot be fully explained only by the conventional image force barrier lowering effect which is also pointed in Ref. [21]. Thus, the SBH reduction with dopant subsitution should be viewed as a results of the interplay between the compensated interface dipole (due to charge transfer at the interface) and the induced image-force barrier lowering.

IV. CONCLUSION

We have investigated the interface morphology dependent SBH in the $NiSi_2$/Si interfaces and its modulation by substitutional dopants using DFT by employing MGGA exchange correlation functional. The SBHs for both electrons and holes were extracted by inspecting the LDOS for the given atomic configuration at the interface. The results agree very well with experiments even with inherent ambiguity in the LDOS method. In addition, we have clearly shown the SBH with (001) Si is significantly lower than (111) Si which strongly supports the interface morphology dependent SBH from experimental observations. Also, we have shown that the n-type and p-type SBH can be significantly reduced for both $NiSi_2$/(001)Si and $NiSi_2$/(111)Si by As and B substitution, respectively, becaused of the interplay between the compensated interface dipole and the induced image forace barrier lowering.

ACKNOWLEDGMENT

The authors would like to thank to Dr. Qun Gao and Dr. Sudarshan Narayanan at GLOBALFOUNDRIES and Dr. Ander Blom at QuantumWise A/S for their valuable discussions and technical supports.

REFERENCES

[1] "International technology roadmap for semiconductors," 2015. [Online]. Available: http://www.itrs.net

[2] J. Tersoff, "Schottky barrier heights and the continuum of gap states," *Physical Review Letters*, vol. 52, no. 6, p. 465, 1984.

[3] J. Robertson, "Band offsets of wide-band-gap oxides and implications for future electronic devices," *Journal of Vacuum Science & Technology B*, vol. 18, no. 3, pp. 1785–1791, 2000.

[4] J. Robertson, "Band offsets, schottky barrier heights, and their effects on electronicdevices," *Journal of Vacuum Science & Technology A*, vol. 31, no. 5, p. 050821, 2013.

[5] R. Tung, A. Levi, J. Sullivan, and F. Schrey, "Schottky-barrier inhomogeneity at epitaxial $NiSi_2$ interfaces on Si (100)," *Physical review letters*, vol. 66, no. 1, p. 72, 1991.

[6] R. Tung, "Schottky barrier heights of single crystal silicides on Si (111)," *Journal of Vacuum Science & Technology B*, vol. 2, no. 3, pp. 465–470, 1984.

[7] H. Fujitani and S. Asano, "Schottky barriers at $NiSi_2$/Si (111) interfaces," *Physical Review B*, vol. 42, no. 3, p. 1696, 1990.

[8] H. Fujitani and S. Asano, "Schottky-barrier height and electronic structure of the Si interface with metal silicides: $CoSi_2$, $NiSi_2$, and YSi_2," *Physical Review B*, vol. 50, no. 12, p. 8681, 1994.

[9] C. Kenney, K.-W. Ang, K. Matthews, M. Liehr, M. Minakais, J. Pater, M. Rodgers, V. Kaushik, S. Novak, S. Gausepohl *et al.*, "Finfet parasitic resistance reduction by segregating shallow Sb, Ge and As implants at the silicide interface," in *VLSI Technology (VLSIT), 2012 Symposium on*. IEEE, 2012, pp. 17–18.

[10] R. T. Lee, T.-Y. Liow, K.-M. Tan, A. E.-J. Lim, H.-S. Wong, P.-C. Lim, D. M. Lai, G.-Q. Lo, C.-H. Tung, G. Samudra *et al.*, "Novel nickel-alloy silicides for source/drain contact resistance reduction in n-channel multiple-gate transistors with sub-35 nm gate length," in *Electron Devices Meeting, 2006. IEDM'06. International*. IEEE, 2006, pp. 1–4.

[11] A. Kinoshita, Y. Tsuchiya, A. Yagishita, K. Uchida, and J. Koga, "Solution for high-performance schottky-source/drain mosfets: Schottky barrier height engineering with dopant segregation technique," in *VLSI Technology, 2004. Digest of Technical Papers. 2004 Symposium on*. IEEE, 2004, pp. 168–169.

[12] G. Das, P. Blöchl, O. Andersen, N. Christensen, and O. Gunnarsson, "Electronic structure and schottky-barrier heights of (111) $NiSi_2$/Si a- and b-type interfaces," *Physical review letters*, vol. 63, no. 11, p. 1168, 1989.

[13] Y. Nishi, T. Yamauchi, T. Marukame, A. Kinoshita, J. Koga, and K. Kato, "Schottky barrier height modulation by atomic dipoles at the silicide/silicon interface," *Physical Review B*, vol. 84, no. 11, p. 115323, 2011.

[14] Q. Gao and J. Guo, "Barrier height determination of silicide-silicon contact by hybrid density functional simulation," *Applied Physics Letters*, vol. 99, no. 18, p. 183110, 2011.

[15] Atomistix ToolKit version 2014.2, QuantumWise A/S (www.quantumwise.com).

[16] K. Stokbro and S. Smidstrup, "Electron transport across a metal-organic interface: Simulations using nonequilibrium green's function and density functional theory," *Physical Review B*, vol. 88, no. 7, p. 075317, 2013.

[17] F. Tran and P. Blaha, "Accurate band gaps of semiconductors and insulators with a semilocal exchange-correlation potential," *Physical Review Letters*, vol. 102, no. 22, p. 226401, 2009.

[18] L. Geng, B. Magyari-Köpe, and Y. Nishi, "Image charge and dipole combination model for the schottky barrier tuning at the dopant segregated metal/semiconductor interface," *Electron Device Letters, IEEE*, vol. 30, no. 9, pp. 963–965, 2009.

[19] N. Nilsson, "An accurate approximation of the generalized einstein relation for degenerate semiconductors," *physica status solidi (a)*, vol. 19, no. 1, pp. K75–K78, 1973.

[20] M. Furno, F. Bonani, and G. Ghione, "Transfer matrix method modelling of inhomogeneous schottky barrier diodes on silicon carbide," *Solid-state electronics*, vol. 51, no. 3, pp. 466–474, 2007.

[21] Y. Jiao, A. Hellman, Y. Fang, S. Gao, and M. Kall, "Schottky barrier formation and band bending revealed by first-principles calculations," *Scientific Reports*, vol. 5, no. 11374, 2015.